WILEY-VCH

Supplementary Information

Constructing Interconnected Gel with Ionic Fluid Channels for AC Line-Filtering

Jie Zhang,[a] *Zhuanpei Wang**[b] *and Xiaowei Yang**[a]

[a] School of Chemistry and Chemical Engineering, Shanghai Jiao Tong University, Shanghai 200240, P. R. China
E-mail: yangxw@sjtu.edu.cn

[b] School of Energy Science and Technology, Longzihu New Energy Laboratory, Zhengzhou Institute of Emerging Industrial Technology, Henan University, Zhengzhou, 450046, P. R. China
E-mail: zhuanpeiwang@henu.edu.cn

Experimental Section

Preparation GO Dispersion: GO aqueous dispersion was prepared by a modified Hummers' method. The obtained brown dispersion was subjected to 40 min of centrifugation at 8500 rpm to remove large GO and any aggregates. Then it was purified by dialysis for 2 weeks to remove the remaining salt impurities for the following experiments. After that, the treated GO dispersion was diluted in deionized water to yield a concentration of 1.0 mg mL^{-1} and then sonicated for 60 min at an amplitude of 40% of the maximum power by a probe sonicator in an ice-water bath (320 W). The resulting dispersion was centrifuged again at 8500 rpm for 40 minutes, and the upper layer liquid was taken to prepare the reaction solution at 0.5 mg mL^{-1}.

Synthesis of rGG^0, rGM and rGG membranes: Briefly, 40 mL 0.5 mg mL^{-1} GO dispersion was mixed with 500 μL ammonia (28 wt.% in H_2O) and 50 μL hydrazine (85 wt.% in H_2O) solution in a 50 mL polytetrafluoroethylene hydrothermal reactor. After being vigorously shaken for several minutes, the reactor was sealed in a stainless-steel reaction kettle and conducted a hydrothermal reaction of 120°C for 3 hours. Then rGG^0 membrane were fabricated by direct-flow vacuum filtration. Briefly, a controlled amount of the as-obtained rGO dispersion was vacuum filtered through a mixed cellulose ester (50 nm pore size, Millipore) filter membrane. When there was no dispersion on the filtrate cake, the filter was pumped for another 60 minutes, and then the obtained rGG^0 film was soaked in deionized water for several times to remove excess ammonia and unreacted hydrazine hydrate. Ultimately, the rGG^0 soaked in 5.0 M H_2SO_4 or 0.05 M H_2SO_4, followed by gentle vacuum drying at 30 °C for 12 h to obtain rGG or rGM.

Synthesis of Different G_xC_y Gels and Electrical Double-Layer Capacitors: First, a 0.5 mg/mL GO dispersion and a 0.5 mg/mL MWCNT dispersion were mixed in various mass ratios, maintaining a total concentration of 0.5 mg/mL. A 40 mL aliquot of the resulting GO/MWCNT hybrid dispersion was mixed with 500 μL of ammonia (28 wt.%) and 50 μL of hydrazine hydrate (85 wt.%) in a 50 mL Teflon-lined hydrothermal autoclave. After vigorous shaking for several minutes, the autoclave was sealed in a stainless-steel shell and subjected to a hydrothermal reaction at 120°C for 3 hours to obtain the reduced GO/MWCNT dispersion. Subsequently, the GxCy gel films (where x and y represent the ratio of GO to MWCNT) were fabricated via vacuum filtration using a diaphragm pump at a pressure of 800 mbar. For instance, the gel film prepared by mixing 32 mL of 0.5 mg/mL GO dispersion with 8 mL of 0.5 mg/mL MWCNT dispersion was designated as G4C1.

Specifically, varying volumes of the reduced GO/MWCNT dispersion were also filtered through a 50 nm pore size mixed cellulose ester membrane. Once the dispersion was completely

filtered, the suction was continued for an additional 60 minutes. The resulting gel films were then immersed in deionized water multiple times to remove excess ammonia and unreacted hydrazine hydrate. Finally, the films were soaked in 5 M H_2SO_4 for 12 hours for thorough infiltration. After gently wiping the surface liquid with filter paper, the gel films were placed in a vacuum oven at 30℃ for 12 hours of mild drying to remove volatile water, yielding the final GxCy electrodes.

The dried film electrodes were washed multiple times with deionized water and subsequently immersed in a 3 M H_2SO_4 electrolyte. The films were gently agitated in the solution to ensure thorough interlayer infiltration of the electrolyte before being transferred onto Pt electrodes. Specifically, the active material side was first lightly pressed onto the Pt current collector, followed by uniform pressing to ensure intimate contact across the entire interface. After being left in the air for 5 minutes, the MCE filter membrane attached to the other side of the electrode material was carefully peeled off using a blade, yielding the Pt-electrode assembly. An NKK-TF4030 separator was then placed on the electrode, and 20 μL of 3 M H_2SO_4 electrolyte was added dropwise. Finally, a symmetrical supercapacitor was assembled by incorporating another identical Pt-electrode assembly.

Material Characterization: The morphology and microstructure of the samples were characterized by a field emission scanning electron microscope (FE-SEM, Apreo 2S, Thermo Fisher). The SEM samples were subjected to a rigorous ion liquid replacement treatment before the test to maintain their original morphological characteristics. The specific steps are as follows: the samples were first subjected to a graded ethanol dehydration series (20%, 40%, 60%, 80%, and 100% v/v) to alleviate osmotic stress and prevent deformation. The dehydrated matrices were then incrementally infiltrated with $EMIMBF_4$/ethanol mixtures of increasing concentration (25%, 50%, 75%, and 100% v/v) to ensure thorough displacement. Following the removal of volatile ethanol residues under low vacuum, the ionic liquid-impregnated gels were obtained. X-ray photoelectron spectroscopy (XPS, ESCALAB Qxi, Thermo Fisher) and Raman (RISE-MAGNA, TESCAN) were used for elemental and defect analysis of samples. X-ray diffraction patterns were collected by a Bruker diffractometer (XRD, D8 Advance) with Cu Kα radiation, λ=1.54 Å.

Electrochemical Measurements & Calculations: The electrochemical performances were evaluated using an electrochemical station (Ivium, Netherland), including cyclic voltammetry (CV), galvanostatic charge-discharge (GCD), electrochemical cycling stability and electrochemical impedance spectroscopy (EIS). EIS measurements were performed from 100 kHz to 100 mHz at an amplitude of 10 mV.

The performance parameters based on the data from electrochemical and EIS measurements are calculated and analyzed concerning other works on filtering capacitors. The real $C^{'}$ (the areal capacitances (C_A) of the EDLCs and volumetric capacitances (C_V) of the electrodes) and imaginary capacitances $C^{''}$ of the device corresponding to the frequency, and the formulas are shown in Equations (1) and (2), respectively:

$$C^{'} = -\frac{z^{''}}{2\pi f|z|^2 X} \quad (1)$$

$$C^{''} = -\frac{z^{'}}{2\pi f|z|^2 X} \quad (2)$$

Where $C^{'}$ is the real capacitance, $C^{''}$ is the imaginary capacitance, $Z^{'}$ is the real impedance, $Z^{''}$ is the imaginary impedance, f is the frequency, $|z|$ is the absolute value of the impedance, and X is the unit parameter selected according to the need, which can be specific area (A_x), or specific volume (V_x).

According to the above formulas, we can get the relation plots of real capacitance ($C^{'}$) and imaginary capacitance (C″) versus frequency (f), which is also a key figure reflecting the nature of the filter capacitor. Under normal circumstances, a maximum point will appear on the plots corresponding to the imaginary capacitance, corresponding to a characteristic frequency (f_0). When the operating frequency is lower than f_0, the capacitance behavior dominates; otherwise, the resistance behavior dominates. The inverse of f_0 is another important characteristic constant (τ_0), which is the time required for discharging a capacitor with an energy efficiency greater than 50%. It was used to evaluate the charge/discharge capability, was calculated using Equation (3):

$$\tau_0 = \frac{1}{f_0} \quad (3)$$

In a 120 Hz AC circuit, the resistor-capacitor (RC) time constant required for the filtering capacitor must be less than 8.3 ms. The formula is shown in Equation (4):

$$\tau_{RC} = R_t * C \quad (4)$$

where τ_{RC} is the RC time constant, R_t is the total resistance, C is the capacitance.

The dissipation factor (DF) with the frequency used to demonstrate high frequency response behavior was calculated by the follwing Equation (5):

$$DF = \frac{|P|}{|Q|} = \frac{C^{''}(f)}{C^{'}(f)} \quad (5)$$

Where $|P|$ and $|Q|$ are real and reactive power components, respectively. $Z^{'}$ is the real impedance, $Z^{''}$ is the imaginary impedance, f is the frequency.

XRD was used to probe the crystallized structure in samples on Bruker D8 Advance with Cu Kα radiation (λ = 0.154 nm, 5° to 50°). Since the samples to be tested are gel films with a large amount of water, this test is only used to calculate the distance between the π-π regions of the sheets, Equation (6):

$$d_{\pi\text{-}\pi} = \frac{\lambda}{2sin\theta} \tag{6}$$

The frequency capacitance loss factor (FCLF) is the proportion of capacitance reduction at high frequencies to compare the loss of capacitance caused by frequency changes, Equation (7):

$$\text{FLCF} = 1 - \frac{C_A^f}{C_A^{f^0}} \tag{7}$$

where $C_A^{f^0}$ and C_A^f are the areal capacitance of initial frequency (f^0 = 0.1 Hz) and calculated frequency (f).

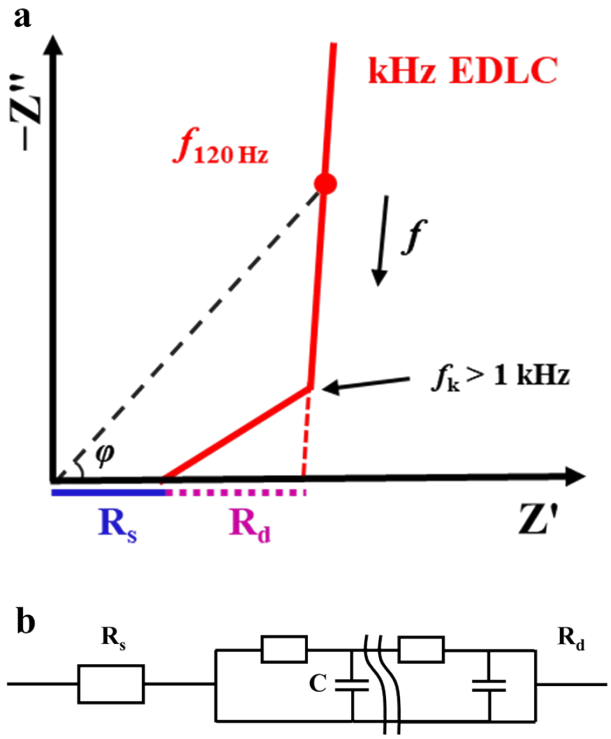

Fig. S1 (a) Nyquist plot of kHz EDLC and (b) corresponding equivalent circuit (C is the capacitance of electrode materials).

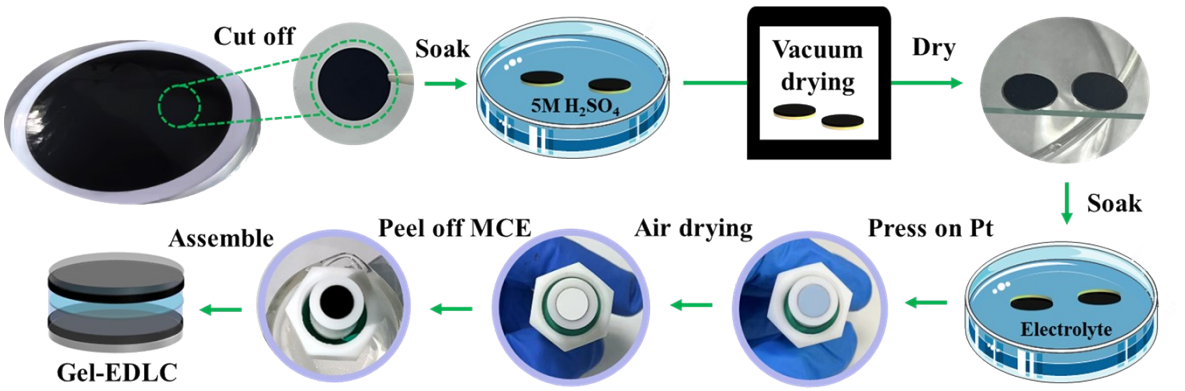

Fig. S2 Assembly process of the symmetric Gel-EDLC based on a wet-gel strategy, encompassing vacuum filtration, volatile component displacement, and transfer-printing.

The as-prepared gel electrodes were thoroughly washed and cut. By carefully displacing 5 M sulfuric acid and evaporating the volatile components, the thickness of the gel electrodes was precisely compressed to half of its original size without inducing the catastrophic pore collapse typically caused by the intense capillary forces in conventional drying methods.

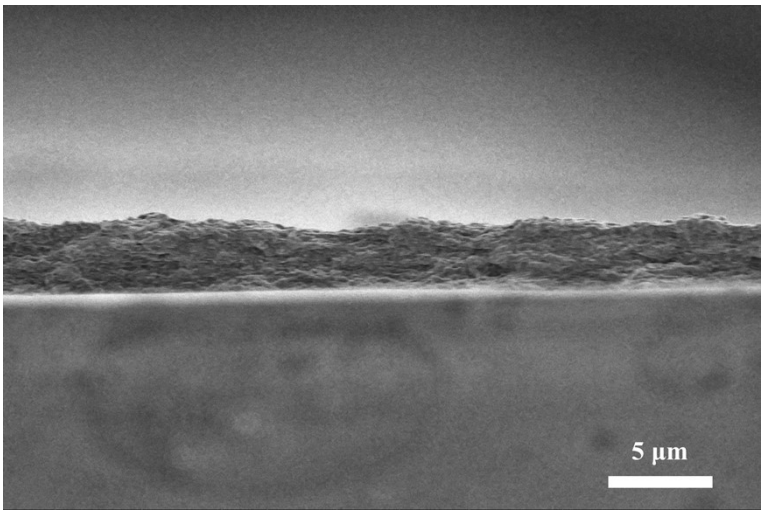

Fig. S3 The cross-section SEM image of rGG (The thickness is ~4.5 micrometers).

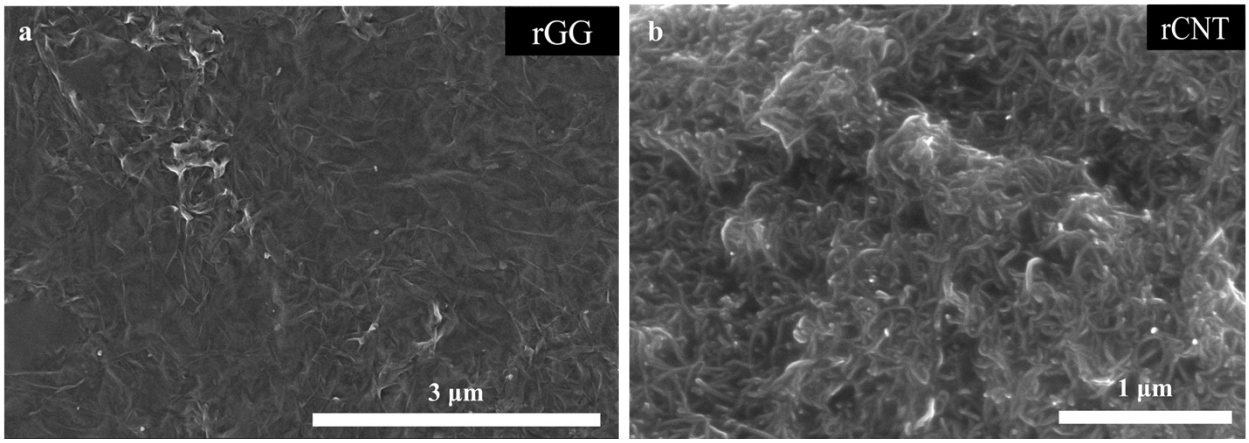

Fig. S4 Surface SEM images of (a) rGG and (b) rCNT gel-membranes.

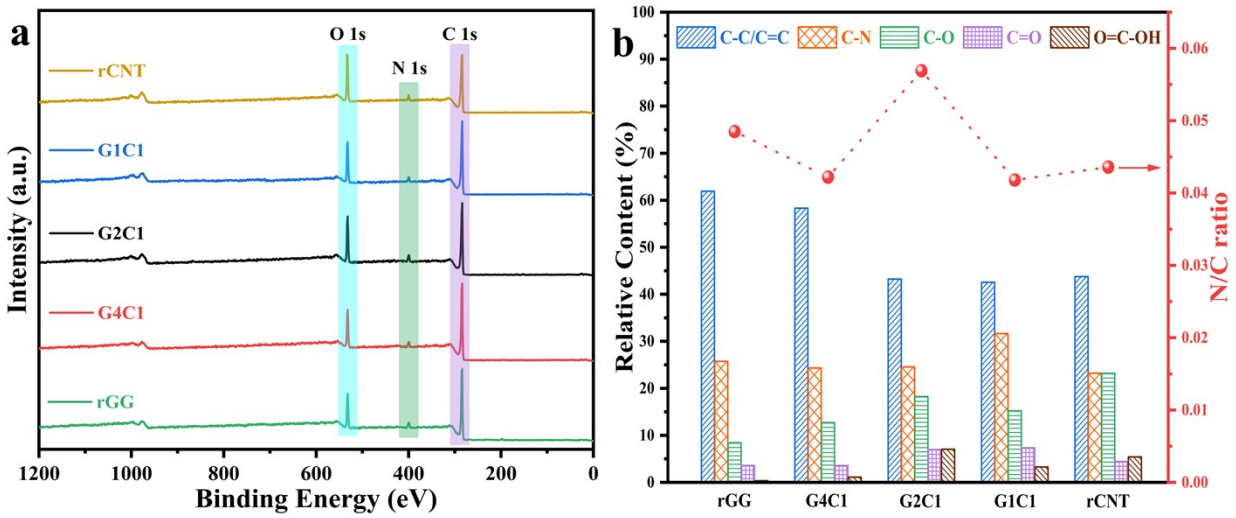

Fig. S5 (a) XPS survey spectra and (b) the corresponding quantitative distribution of chemical bonds and N/C atomic ratios of rGG, G4C1, G2C1, G1C1 and rCNT membranes, respectively.

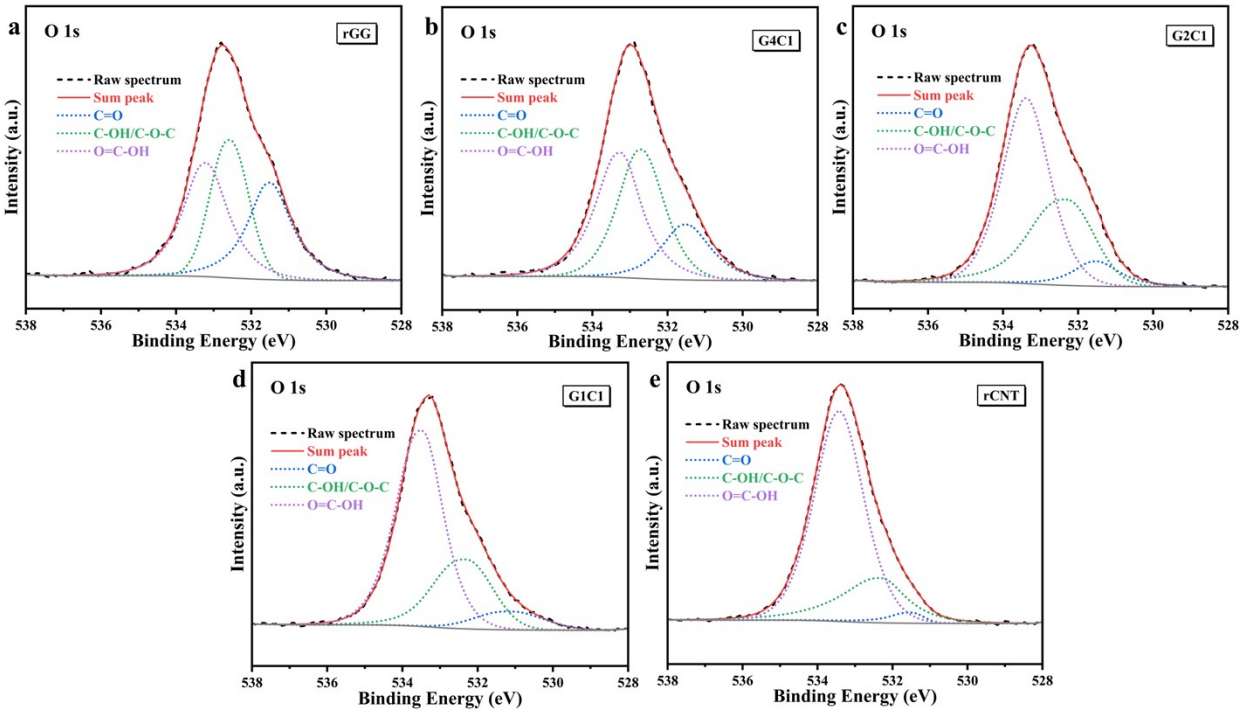

Fig. S6 O 1s XPS spectra of (a) rGG, (b) G4C1, (c) G2C1, (d) G1C1 and (e) rCNT membranes, respectively.

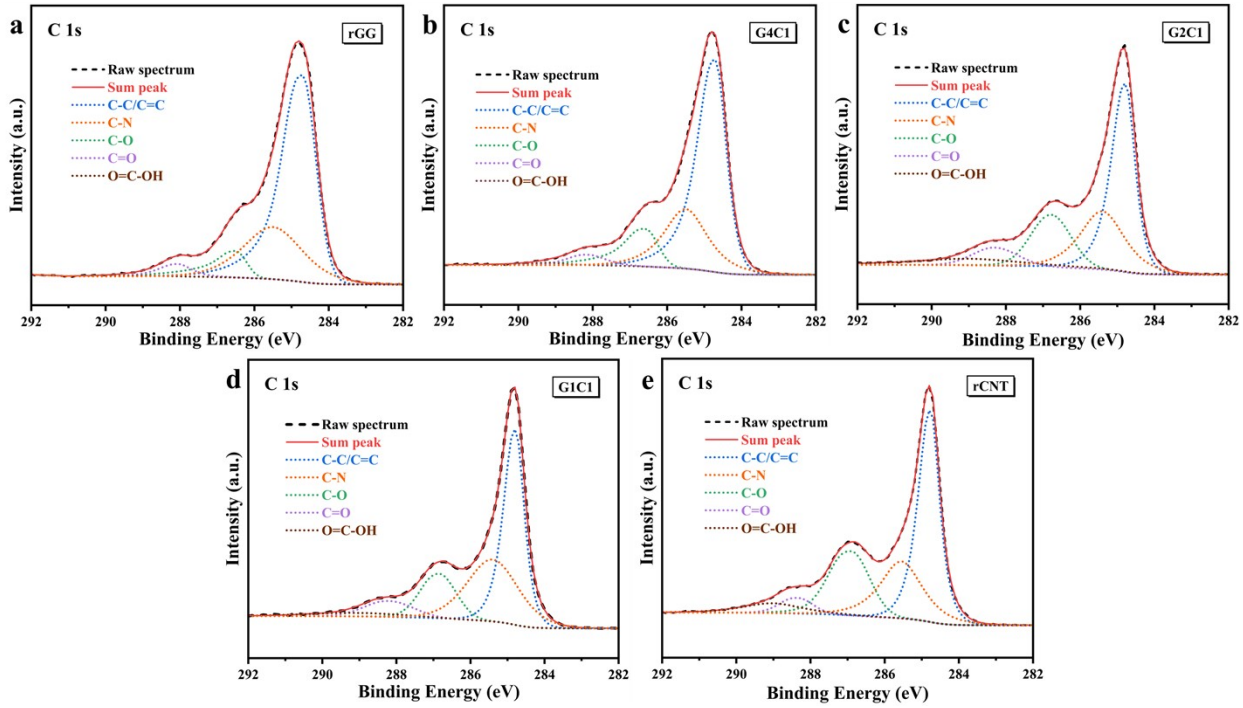

Fig. S7 C 1s XPS spectra of (a) rGG, (b) G4C1, (c) G2C1, (d) G1C1 and (e) rCNT membranes, respectively.

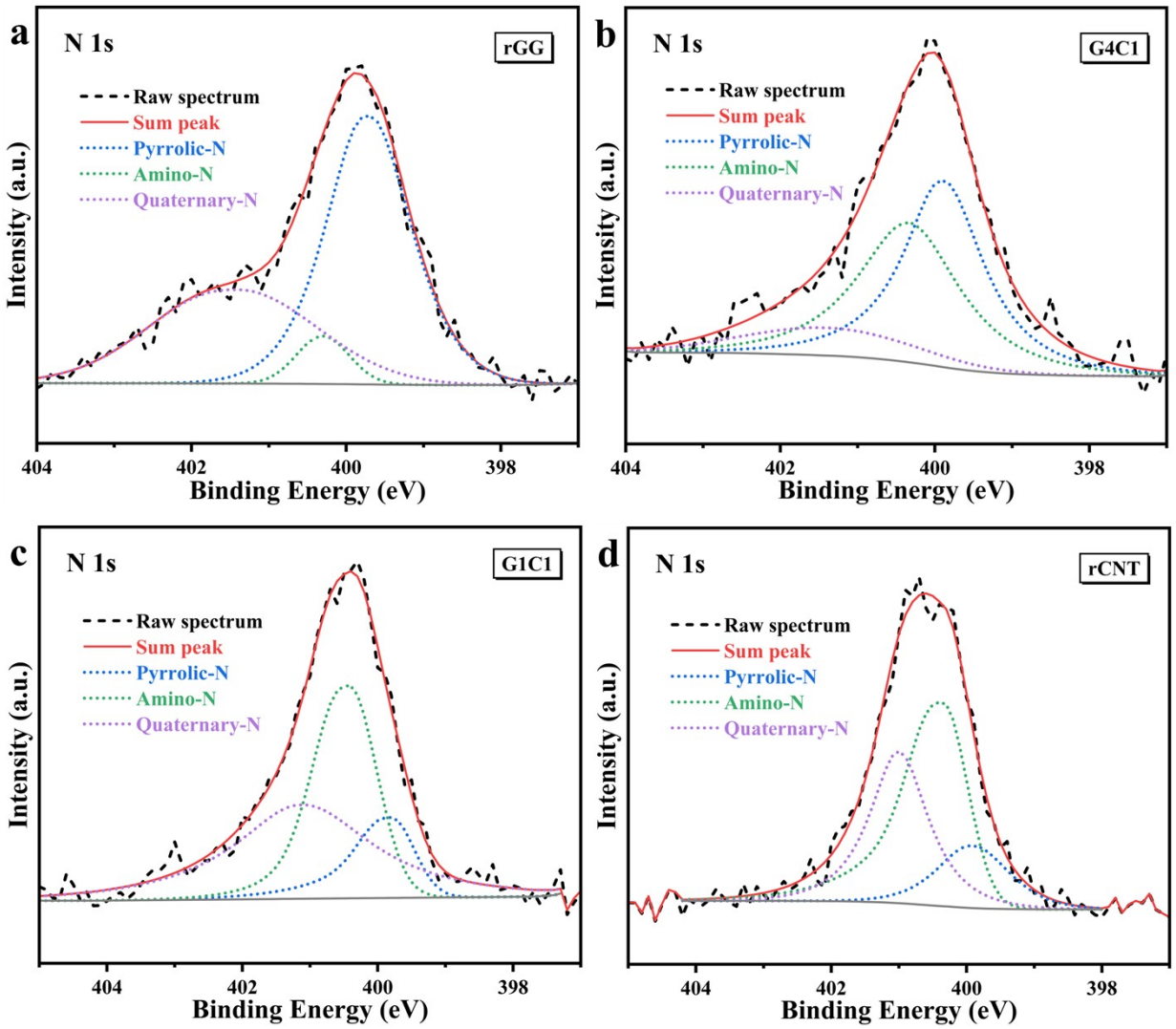

Fig. S8 N 1s XPS spectra of (a) rGG, (b) G4C1, (c) G1C1 and (d) rCNT membranes, respectively.

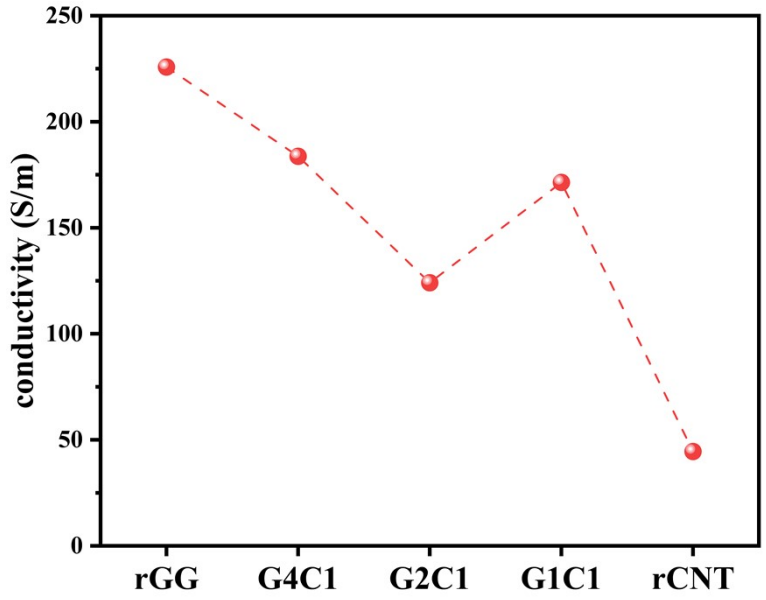

Fig. S9 Conductivity of rGG, G4C1, G2C1, G1C1 and rCNT membranes.

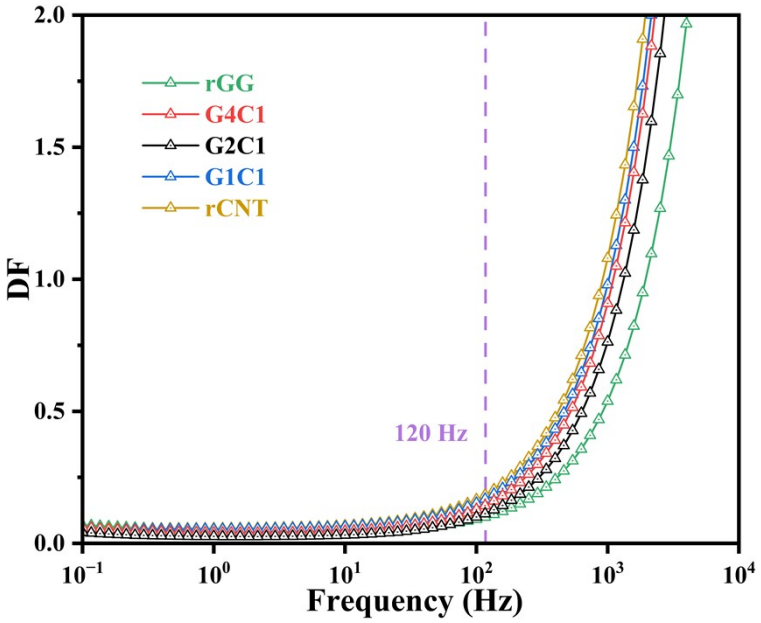

Fig. S10 DF versus frequency of the five gels based EDLCs.

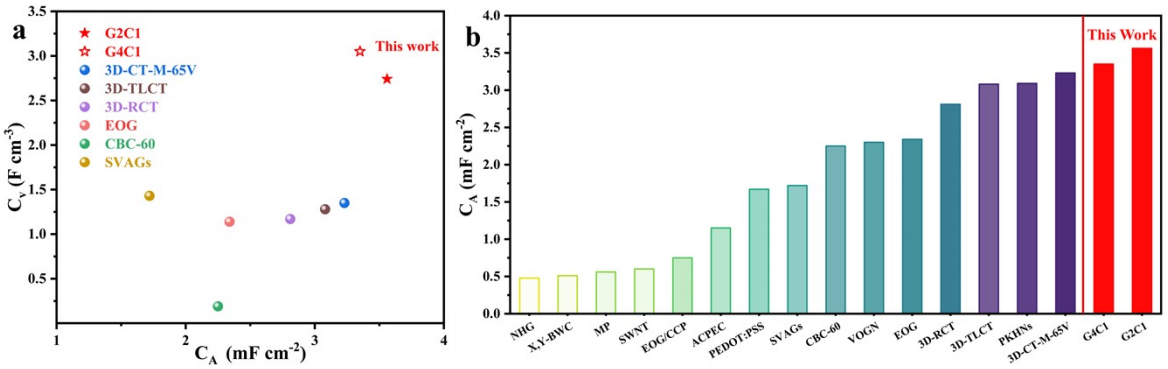

Fig. S11 (a) C_V and (b) C_A of GxCy based EDLCs against state-of-the-art sandwich filtering capacitors in literature ($-\varphi > 80°$).